

An integral-like numerical approach for solving Burgers' equation

Somrath Kanoksirirath^a,

^a*NSTDA Supercomputer Center (ThaiSC), National Science and Technology
Development Agency (NSTDA), Pathum Thani, 12120, Thailand*

Abstract

An unconventional approach is applied to solve the one-dimensional Burgers' equation. It is based on spline polynomial interpolations and Hopf-Cole transformation. Taylor expansion is used to approximate the exponential term in the transformation, then the analytical solution of the simplified equation is discretized to form a numerical scheme, involving various special functions. The derived scheme is explicit and adaptable for parallel computing. However, some types of boundary condition cannot be specified straightforwardly. Three test cases were employed to examine its accuracy, stability, and parallel scalability. In the aspect of accuracy, the schemes employed cubic and quintic spline interpolation performs equally well, managing to reduce the ℓ_1 , ℓ_2 and ℓ_∞ error norms down to the order of 10^{-4} . Due to the transformation, their stability condition $\nu\Delta t/\Delta x^2 > 0.02$ includes the viscosity/diffusion coefficient ν . From the condition, the schemes can run at a large time step size Δt even when grid spacing Δx is small. These characteristics suggest that the method is more suitable for operational use than for research purposes.

Keywords: Burgers' equation, Integral-like approach, Hopf-Cole transformation, Explicit scheme, parallel scalability
2000 MSC: 35Q35,

1. Introduction

The partial differential equation (PDE) of the form

$$\frac{\partial u}{\partial t} + u \frac{\partial u}{\partial x} = \nu \frac{\partial^2 u}{\partial x^2} \quad (1.1)$$

is called one-dimensional Burgers' equation. It models physical transport phenomena in fluid flows, turbulence, traffic flows and other areas [1]. It is a vital part of Navier-Stokes equations where u represents the velocity of the fluid and ν is a positive viscosity/diffusion constant. The equation forms the core of computational fluid dynamics, weather models, ocean models, and hydrodynamic models.

The second term, uu_x , is non-linear, which hinders the development of simple, stable and accurate numerical methods for solving various physics equations in practice. This study proposes an approach to address this non-linear term while keeping the scheme simple and explicit, as highly complex schemes often suffer from poor parallel scalability, limiting their practical use. Additionally, in contrast to most explicit schemes that have severe stability conditions resulting in higher computational costs, our scheme is stable even at large time step sizes.

The solution of Burgers' equation can be obtained analytically by converting it to a diffusion equation, $\phi_t = \nu\phi_{xx}$, using Hopf-Cole transform, Eqs. (1.2) and (1.3), and then solving it using Fourier transform or other methods. However, this approach is inconvenient and unsuitable for arbitrary initial and boundary conditions commonly encountered in practice. Therefore, several numerical schemes have been developed.

$$\phi(x, t) = \exp\left(\frac{-1}{2\nu} \int_{0^+}^x u(\xi, t) d\xi\right) \quad (1.2)$$

$$u = -2\nu \frac{\phi_x}{\phi} \quad (1.3)$$

The standard numerical approach to tackle the non-linear term is to linearize it by assuming that u in uu_x is locally constant, as done in previous works such as [2, 3, 4, 5, 6, 7, 8]. However, this approach usually has limitations, particularly in terms of accuracy. Huang and Abduwali [6] successfully developed an explicit and unconditionally stable scheme using this assumption. Another approach is to rewrite the non-linear term as $(u^2)_x$ and solve it accordingly as in [9, 10, 11, 12, 13, 14]. However, these methods often involve complicated, iterative or implicit schemes that require solving a large set of linear equations, which can limit computational speed and parallel scalability of the programs.

On the other hand, some researchers, e.g., [15, 16, 17, 18, 19, 20, 21, 22, 23, 24], have applied numerical Hopf-Cole transformation and solved the resulting diffusion equation instead. Advanced schemes have been employed

to accurately diffuse exponential profiles generated by the Hopf-Cole transformation, while the transformation itself is generally approximated using a finite number of terms of its infinite series form or integrated numerically using Gaussian quadrature.

In terms of numerical procedures, the relatively expensive finite element method is widely employed [25, 26, 27, 28, 3, 16, 14, 24], as well as the Galerkin approach with cubic polynomials or others basis functions [2, 29, 4, 30, 10, 5, 11, 17, 31, 32, 7]. Nevertheless, several studies have used the conventional finite difference method [6, 12, 15, 18, 19, 20, 8], with most of them being implicit schemes. Additionally, Gao et al. [33] applied a particle-based scheme to the Burgers' equation. To speed up implementation, Kumar et al. [34] developed a hybrid predictor-corrector scheme, while an artificial neural network was adopted to accelerate a prior Galerkin approach in [35].

In this paper, we introduce an integral-like approach that mimics mathematical transformations and temporal integration to advance the numerical solution in time. In contrast to finite discretization, we employ spline interpolation to represent gridded data as a continuous function. The general idea of this approach is explained in Section 2. In Section 3, the time-stepping method used in solving the diffusion equation is described as an example and as an indispensable part of the scheme for solving Burgers' equation. In Section 4, the numerical Hopf-Cole transformation is explained and the entire scheme is composed with additional remarks on programming aspect. In Section 5, the results of several numerical experiments are shown, including an example of solving Burgers'-Fisher equation. Conclusions are presented in Section 6.

2. Integral-like approach

The proposed integral-like approach is different from conventional methods in both numerical differentiation in space and numerical forwarding scheme in time. To solve a PDE, our data grid contains not only the necessary field variables but also their derivatives, so that the variables can be represented as a continuous function using spline polynomial interpolation between adjacent grid points. To advance the variables in time, mathematical procedures along with additional approximations, based on the corresponding analytical solution, are emulated using the known continuous spline polynomial function. The derivatives also need to be updated in time. Initializing the derivatives using a finite difference method has been found to

Table 1: Integral-like schemes with their associated spline polynomial interpolations P_j for u, u_x and u_{xx} between x_j and x_{j+1} where $y = x - x_j$ and $0 \leq y < \Delta x$

Scheme	Local spline polynomial $P_j(y)$	Data grid
Linear (LG)	$a_j y + b_j$	u
Cubic (CG)	$a_j y^3 + b_j y^2 + c_j y + d_j$	u
	$3a_j y^2 + 2b_j y + c_j$	u_x
Quintic (QG)	$a_j y^5 + b_j y^4 + c_j y^3 + d_j y^2 + e_j y + f_j$	u
	$5a_j y^4 + 4b_j y^3 + 3c_j y^2 + 2d_j y + e_j$	u_x
	$20a_j y^3 + 12b_j y^2 + 6c_j y + 2d_j$	u_{xx}

be sufficient. Since we can split terms in a PDE and solve more but simpler PDEs successively, as discussed in [36], the approach can be applied to any Burger's-type equation. In Section 5, a Burgers'-Fisher equation, $u_t + uu_x = \nu u_{xx} - 3u(1-u)(1-2u)$, is split and solved as an example.

In this paper, we investigate integral-like methods that utilize linear, cubic and quintic spline interpolations. These methods will be referred to as linear grid scheme (LG), cubic grid scheme (CG) and quintic grid scheme (QG) respectively, as in Table 1. For the cubic and quintic schemes, the second-order central finite difference is used to initialize u_x and u_{xx} , except at the two end points where the first-order forward and backward finite difference are employed instead.

To forward the numerical solution of the Burgers' equation in time, the Hopf-Cole transformation is applied numerically, the resulting diffusion equation is solved in the Hopf-Cole space and then converted back to the normal space. The application of the integral-like approach to the diffusion equation is discussed first to familiarize readers with the general idea of the method. It is worth noting that the integral-like approach is an explicit scheme that incorporates mathematical formulas and is equivalent to a Semi-Lagrangian method when applied to the linear advection equation.

3. Method for linear diffusion

The linear diffusion equation, $\phi_t = \nu \phi_{xx}$, where ν is a positive diffusion constant, can be solved analytically using the Fourier transform. This ap-

proach is discussed in textbooks such as [37] and [38]. The analytical solution is

$$\phi(x, t) = \int_{-\infty}^{\infty} \frac{1}{\sqrt{4\pi\nu t}} \exp\left(-\frac{(x-\xi)^2}{4\nu t}\right) \phi(\xi, 0) d\xi \quad (3.1)$$

with analytical boundary conditions $\phi(\infty, t) = \phi(-\infty, t) = 0$.

The time-stepping scheme of the integral-like approach can be derived from Eq. (3.1) by substituting the spline polynomial function $P_j(y, t)$ and changing the time interval. In the case of the cubic scheme (CG) with equally-spacing grid points, Eq. (3.1) becomes

$$\begin{aligned} \phi(x_i, t + \Delta t) &= \sum_{j=-\infty}^{\infty} \int_0^{\Delta x} \frac{1}{\sqrt{4\pi\nu\Delta t}} \exp\left(-\frac{(x_i - (\xi_j + y))^2}{4\nu\Delta t}\right) P_j(y, t) d(\xi_j + y) \\ &\approx \frac{1}{\sqrt{4\pi\nu\Delta t}} \sum_{|\ell_{i,j}| \leq 5\sigma} \int_0^{\Delta x} \exp\left(-\frac{(y + \ell_{i,j})^2}{4\nu\Delta t}\right) (a_j y^3 + b_j y^2 + c_j y + d_j) dy \end{aligned} \quad (3.2)$$

Due to the Gaussian decay term, the summation range can be limited to j such that the relative distance $\ell_{i,j} \equiv \xi_j - x_i$ is within a margin of five standard deviations, i.e., $5\sigma = 5\sqrt{2\nu\Delta t}$, which is chosen for this paper.

It was found experimentally that all three methods are numerically stable as long as the marginal range of 5σ is larger than the grid spacing Δx . This is evidenced in Figure 7. Mathematically, the condition is equivalent to $d \geq 0.02$, where $d = \nu(\Delta t)/(\Delta x)^2$ is a non-dimensional diffusion number. Interestingly, the stability condition for these methods is reversed compared to the stability condition of explicit finite difference schemes. Since the 5σ length is an estimation, the value 0.02 is not exact. Notably, the stability condition is independent of u .

Due to the summation of j within the marginal range, the time complexity of the integral-like method is $\mathcal{O}((5\sigma/\Delta x) n_x n_t) \sim \mathcal{O}((\sqrt{\nu\Delta t}/\Delta x) n_x n_t) \sim \mathcal{O}(\sqrt{\nu} n_x^2 n_t^{1/2})$, where n_x is the number of grid points and n_t is the total number of time step. Evidently, the complexity of the algorithm is not linear.

Another implication of the marginal range is that the boundary conditions may have to be specified by a small set of points, instead of a single point exactly at the boundary. For example, in the case of periodic boundary condition, the required outside point $-j$ on the left of the considered domain corresponds to the inside point $n - j$. Similarly, the values at the outside point $n_x + j$ on the right are that of the j -th point. For Dirichlet and

no-flux boundary conditions, reflected points or their mirror images can be used. Adding extra grid points to both ends can keep the implementation simple and is adopted here, as it also matches with the domain decomposition method for parallelization.

Next, to quantify Eq. (3.2), the indefinite integral of the form, $\int y^m \exp(-(y+\ell)^2/\delta) dy$, where m is a positive integer, is evaluated recursively using Eqs. (3.3) - (3.5), which derived by applying integration by parts.

$$\begin{aligned} PG_m &\equiv \int y^m \exp\left(-\frac{(y+\ell)^2}{\delta}\right) dy \\ &= (m-1) \frac{\delta}{2} PG_{m-2} - \ell PG_{m-1} - \frac{\delta}{2} y^{m-1} \exp\left(-\frac{(y+\ell)^2}{\delta}\right) \end{aligned} \quad (3.3)$$

where

$$PG_0 = \frac{\sqrt{\pi\delta}}{2} \left[\operatorname{erf}\left(\frac{y+\ell}{\sqrt{\delta}}\right) - \operatorname{erf}\left(\frac{\ell}{\sqrt{\delta}}\right) \right] \quad (3.4)$$

$$PG_1 = -\frac{\ell\sqrt{\pi\delta}}{2} \left[\operatorname{erf}\left(\frac{y+\ell}{\sqrt{\delta}}\right) - \operatorname{erf}\left(\frac{\ell}{\sqrt{\delta}}\right) \right] - \frac{\delta}{2} \left[\exp\left(-\frac{(y+\ell)^2}{\delta}\right) - \exp\left(-\frac{\ell^2}{\delta}\right) \right] \quad (3.5)$$

On the other hand, the coefficients of the cubic spline polynomial function $P_j(y)$, i.e., a_j, b_j, c_j and d_j , are found by solving Eqs. (3.6) - (3.9) at each time step. These coefficients are analytically solved beforehand to speed up the program.

$$P_j(\Delta x, t) = \phi_{j+1} = a_j(\Delta x)^3 + b_j(\Delta x)^2 + c_j(\Delta x) + d_j \quad (3.6)$$

$$\partial_x P_j(\Delta x, t) = \partial_x \phi_{j+1} = 3a_j(\Delta x)^2 + 2b_j(\Delta x) + c_j \quad (3.7)$$

$$P_j(0, t) = \phi_j = d_j \quad (3.8)$$

$$\partial_x P_j(0, t) = \partial_x \phi_j = c_j \quad (3.9)$$

We denote $\partial_x \phi_j$ as the first derivative of ϕ at grid point j . These derivatives are stored in a data grid and are updated by using Eq. (3.10), which derived

by differentiating Eq. (3.2) with respect to x_i .

$$\begin{aligned}
\frac{\partial}{\partial x_i} \phi(x_i, t + \Delta t) &= \frac{1}{\sqrt{4\pi\nu\Delta t}} \sum_{|\ell_{i,j}| \leq 5\sigma} \int_0^{\Delta x} \left[\frac{\partial(\xi_j - x_i)}{\partial x_i} \frac{\partial}{\partial \ell_{i,j}} \exp\left(-\frac{(y + \ell_{i,j})^2}{4\nu\Delta t}\right) \right] \\
&\quad \left(a_j y^3 + b_j y^2 + c_j y + d_j \right) dy \\
&= \frac{1}{\sqrt{4\pi\nu\Delta t}} \sum_{|\ell_{i,j}| \leq 5\sigma} \int_0^{\Delta x} \left[(-1) \left(\frac{-2(y + \ell_{i,j})}{4\nu\Delta t} \right) \exp\left(-\frac{(y + \ell_{i,j})^2}{4\nu\Delta t}\right) \right] \\
&\quad \left(a_j y^3 + b_j y^2 + c_j y + d_j \right) dy \\
&= \frac{1}{(2\nu\Delta t)\sqrt{4\pi\nu\Delta t}} \sum_{|\ell_{i,j}| \leq 5\sigma} \int_0^{\Delta x} \exp\left(-\frac{(y + \ell_{i,j})^2}{4\nu\Delta t}\right) \\
&\quad \left(a_j y^4 + (b_j + \ell_{i,j}a_j)y^3 + (c_j + \ell_{i,j}b_j)y^2 + (d_j + \ell_{i,j}c_j)y + \ell_{i,j}d_j \right) dy
\end{aligned} \tag{3.10}$$

Hence, Eqs. (3.2) and (3.10) together form the complete time-stepping method for the integral-like cubic scheme. Their computation is facilitated by Eqs. (3.3) - (3.9). The derivation of the linear scheme and the quintic scheme follows a similar approach as the cubic scheme, but with a different form of spline polynomial $P_j(y)$ substituted in, and with a different number of data grids to be stored and iterated in time.

4. Method for Hopf-Cole transformation

For the cubic scheme, the first step in performing the Hopf-Cole transformation, changing u to ϕ (Eq. 1.2), is to compute the integral of u in Eq.

(4.1).

$$\begin{aligned}
\text{Int}(u) &\equiv \int_{0'}^{x_i} u(\xi, t) d\xi = \sum_{j=0}^{i-1} \int_0^{\Delta x} P_j(\xi, t) d\xi \\
&= \sum_{j=0}^{i-1} \int_0^{\Delta x} \left(a_j \xi^3 + b_j \xi^2 + c_j \xi + d_j \right) d\xi \\
&= \sum_{j=0}^{i-1} a_j \frac{(\Delta x)^4}{4} + b_j \frac{(\Delta x)^3}{3} + c_j \frac{(\Delta x)^2}{2} + d_j (\Delta x)
\end{aligned} \tag{4.1}$$

Then, the exponent $-(1/2\nu) \text{Int}(u)$ in Eq. (1.2) is represented as a quintic spline polynomial function using $\text{Int}(u)$, u and u_x . The quintic coefficients are found by solving six linear equations developed analogously to Eqs. (3.6) - (3.9).

Then, for a quintic polynomial Q_i of the i -th segment, the value of ϕ between x_i and x_{i+1} is written as a Taylor series T_i of $\exp(Q_i)$. In our implementation, the number of terms in the Taylor series are varied adaptively, up to 16 terms, to ensure that the deviation of T_i is less than 0.01%. The resulting ϕ or T_i , which satisfying the diffusion equation, is then solved using the method discussed in Section 3.

On the other hand, the Hopf-Cole transformation from ϕ to u in Eq. (1.3) is done by direct substitution. For example, u and u_x of the cubic scheme are deduced from ϕ , ϕ_x and ϕ_{xx} by using Eqs. (4.2).

$$u_i = -2\nu \left(\frac{\partial_x \phi_i}{\phi_i} \right), \quad \partial_x u_i = -2\nu \left(\frac{\phi_i (\partial_x^2 \phi_i) - (\partial_x \phi_i)^2}{\phi_i^2} \right) \tag{4.2}$$

To sum up, an integral-like scheme for solving Burgers' equation consists of the following components: (1) Numerical Hopf-Cole integration scheme for transforming from u space to ϕ space, (2) Numerical diffusion scheme for advancing $\phi(x, t)$ and its required derivatives to $\phi(x, t + \Delta t)$, (3) Numerical Hopf-Cole differentiation scheme for transforming $\phi(x, t + \Delta t)$ and its derivatives back to u space, and (4) Spline interpolation method for representing discrete data points as a continuous function for the computation in (1)-(3). One complete time iteration step Δt for solving Burgers' equation is composed of (1), (2) and (3). In addition, a finite difference scheme is employed for computing the initial derivatives such as

$u_x(x, t_0)$ from $u(x, t_0)$. Our source code is publicly available on GitHub (<https://github.com/SKanoksi>).

According to our implementation, because the numerical Hopf-Cole integration step involves rapid exponential decay/growth, numerical round-off error must be carefully minimized. At least double-precision floating-point data type may be a minimum. Moreover, additional memory allocation is required for the derivatives of the cubic scheme and the quintic scheme, resulting in space complexity of $\mathcal{O}(4n_x)$ and $\mathcal{O}(6n_x)$ respectively. The common factor of 2 is because a temporary array is needed for keeping updated value at each position, before entirely transferred to the primary array in the final step. For our current implementation, another n_x array is used to temporarily store $\text{Int}(u)$.

An implementation of an adaptive grid was explored, where grid points are redistributed based on the path length of u , numerically approximated using Gaussian quadrature. However, the numerical solution was found to be less accurate due to numerical errors introduced when repeatedly rearranging the grids. Therefore, our unsuccessful implementation of the adaptive grid is briefly noted in this paper to inform the possibility that adaptive grid may not improve integral-like schemes in general.

5. Numerical experiment

In this section, four example cases are used to evaluate the integral-like methods in Table 1. The accuracy of the methods is tested using Example 1 and 2, while numerical stability and parallel scalability are evaluated using Example 3. Example 4 investigates the viability of the split approach for more complicated problems.

To quantify the accuracy of the schemes when comparing with exact/analytical solutions $f(x)$, the ℓ_1 , ℓ_2 and ℓ_∞ error norms are adopted. These error norms

are calculated as shown below, for equally-spacing grid.

$$\ell_1(u) = \frac{\sum_{j=0}^n |u_j - f(x_j)|}{\sum_{j=0}^n |f(x_j)|}, \quad (5.1)$$

$$\ell_2(u) = \frac{\sqrt{\sum_{j=0}^n (u_j - f(x_j))^2}}{\sqrt{\sum_{j=0}^n f(x_j)^2}}, \quad (5.2)$$

$$\ell_\infty(u) = \frac{\max |u_j - f(x_j)|}{\max |f(x_j)|} \quad (5.3)$$

Example 1. Burgers' equation (Eq. 1.1) with the initial condition

$$u(x, 0) = \sin(\pi x) \quad (5.4)$$

and the exact solution

$$u(x, t) = \frac{4\pi\nu \sum_{k=1}^{\infty} k A_k \sin(k\pi x) \exp(-k^2\pi^2\nu t)}{A_0 + 2 \sum_{k=1}^{\infty} A_k \cos(k\pi x) \exp(-k^2\pi^2\nu t)} \quad (5.5)$$

where

$$A_k = \int_0^1 \cos(k\pi x) \exp\left(\frac{\cos(\pi x) - 1}{2\pi\nu}\right) dx \quad (5.6)$$

are considered. Unlike in [33] and [39], periodic boundary conditions are employed.

The exact solution and numerical results are displayed in Figure 1 for $\nu = 0.01$, $\Delta x = 0.02$, and $\Delta t = 0.005$, while the numerical values at some grid points are given in Table 2. The error norms for four different pairs of Δx and Δt are shown in Table 3.

From the results, the linear scheme (LG) always performs the worst, while the cubic scheme (CG) and the quintic scheme (QG) are relatively comparable. For CG and QG, as the grid spacing and time step size are reduced, the error norms may not further decrease as seen in Figure 4, where Δx is varied from 0.005 to 0.04. This behavior may be caused by truncation error introduced when approximating exp and erf functions, which are frequently used in the schemes. As a result, the order of accuracy of CG and QG remains nearly unchanged, while LG is approximately second-order accurate, but probably becomes constant at around $\ell_2 = 10^{-3}$ as well.

Table 2: Numerical results and exact solution of Example 1 at $t = 1.0$ using $\nu = 0.1$ and $\Delta t = 0.01$

Position	Δx	LG	CG	QG	Exact
0.1	0.02	0.065558	0.066306	0.066305	0.066316
	0.01	0.066101	0.066284	0.066283	
0.2	0.02	0.129578	0.131189	0.131187	0.131209
	0.01	0.130750	0.131145	0.131144	
0.3	0.02	0.190039	0.192755	0.192752	0.192786
	0.01	0.192020	0.192689	0.192687	
0.4	0.02	0.243809	0.247999	0.247995	0.248041
	0.01	0.246874	0.247910	0.247908	
0.5	0.02	0.285749	0.291864	0.291859	0.291916
	0.01	0.290232	0.291752	0.291749	
0.6	0.02	0.307656	0.316005	0.316000	0.316068
	0.01	0.313784	0.315876	0.315872	
0.7	0.02	0.297804	0.308022	0.308017	0.308089
	0.01	0.305304	0.307884	0.307880	
0.8	0.02	0.243417	0.253657	0.253653	0.253718
	0.01	0.250927	0.253533	0.253529	
0.9	0.02	0.139279	0.146027	0.146025	0.146065
	0.01	0.144223	0.145951	0.145949	

Table 3: Error norms of Example 1 at $t = 1.0$ using $\nu = 0.1$.

Scheme	Δx	Δt	d	ℓ_1	ℓ_2	ℓ_∞
LG	0.02	0.0200	5.0	1.35e − 02	1.46e − 02	1.72e − 02
	0.02	0.0100	2.5	2.64e − 02	2.85e − 02	3.35e − 02
	0.01	0.0100	10.0	7.19e − 03	7.75e − 03	9.07e − 03
	0.01	0.0025	2.5	2.70e − 02	2.92e − 02	3.42e − 02
CG	0.02	0.0200	5.0	4.25e − 04	4.33e − 04	4.56e − 04
	0.02	0.0100	2.5	1.97e − 04	2.00e − 04	2.11e − 04
	0.01	0.0100	10.0	6.07e − 04	6.16e − 04	6.46e − 04
	0.01	0.0025	2.5	8.27e − 04	8.39e − 04	8.76e − 04
QG	0.02	0.0200	5.0	4.40e − 04	4.48e − 04	4.72e − 04
	0.02	0.0100	2.5	2.12e − 04	2.15e − 04	2.26e − 04
	0.01	0.0100	10.0	6.18e − 04	6.28e − 04	6.58e − 04
	0.01	0.0025	2.5	8.97e − 04	9.10e − 04	9.50e − 04

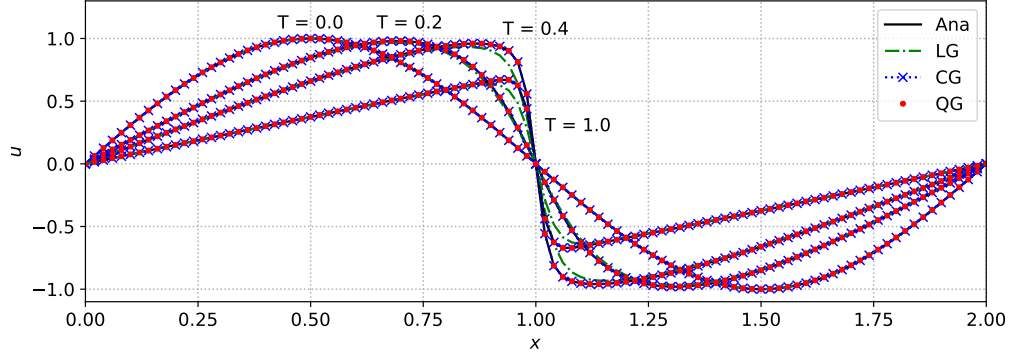


Figure 1: Numerical solutions and exact solution of Example 1: $\nu = 0.01$, $\Delta x = 0.02$, and $\Delta t = 0.005$

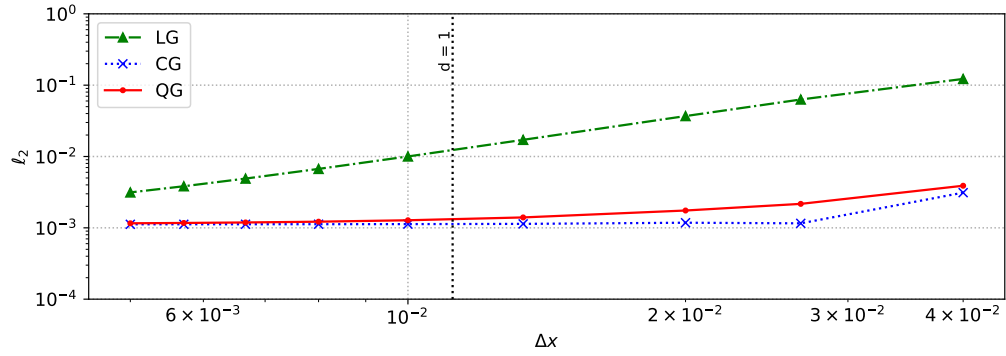


Figure 2: ℓ_2 error norm of Example 1 as a function of Δx using $\nu = 0.1$, $\Delta t = 0.0125$ and $n_t = 100$.

Example 2. Burgers' equation (Eq. 1.1) with the Dirichlet boundary condition

$$u(0, t) = u(1.2, t) = 0 \quad (5.7)$$

and the exact solution

$$u(x, t) = \frac{x/t}{1 + \sqrt{t/t_0} \exp(x^2/4\nu t)} \quad (5.8)$$

where $t \geq 1$ and $t_0 = \exp(0.125/\nu)$ are considered as in [40], [33] and [39]. In our case, the Dirichlet boundary conditions are modeled using the inverted reflection of the solution.

The results of this example, using $\nu = 0.005$, $\Delta x = 0.02$ and $\Delta t = 0.02$, are shown in Figure 3 and Table 4, while Table 5 and Figure 4 provide more insight on their order of accuracy. The results in Figure 4 exhibit similar features as in Figure 2 of previous example, except for the oscillation of CG and QG at small Δx . The swing may be due to the accumulation of errors, similar to Runge's and/or Gibbs phenomenon near the steep slope. This behavior does not occur in Example 1, probably because the abrupt change is stationary at the grid point $x = 0$, while, in this example, the change is not always on a grid points as Δx is varied.

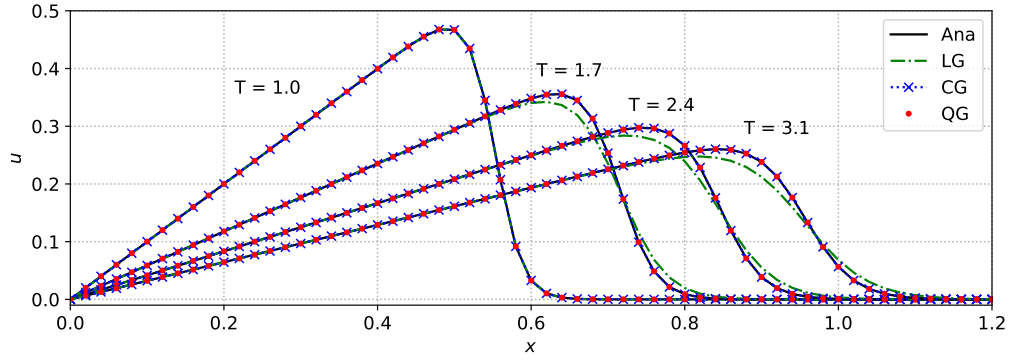


Figure 3: Numerical solutions and exact solution of Example 2: $\nu = 0.005$, $\Delta x = 0.02$ and $\Delta t = 0.02$

Table 4: Numerical results and exact solution of Example 2 at $t = 2.4$ using $\nu = 0.005$ and $\Delta t = 0.02$

Position	Δx	LG	CG	QG	Exact
0.1	0.02	0.041664	0.041663	0.041662	0.041667
	0.01	0.041665	0.041665	0.041665	
0.2	0.02	0.083328	0.083328	0.083326	0.083333
	0.01	0.083331	0.083331	0.083330	
0.3	0.02	0.124995	0.124997	0.124994	0.125000
	0.01	0.124996	0.124996	0.124996	
0.4	0.02	0.166648	0.166661	0.166656	0.166665
	0.01	0.166659	0.166660	0.166659	
0.5	0.02	0.208207	0.208312	0.208305	0.208318
	0.01	0.208299	0.208311	0.208309	
0.6	0.02	0.248953	0.249808	0.249797	0.249816
	0.01	0.249681	0.249806	0.249804	
0.7	0.02	0.281531	0.288475	0.288445	0.288472
	0.01	0.287090	0.288458	0.288454	
0.8	0.02	0.239172	0.266132	0.266155	0.266228
	0.01	0.258598	0.266184	0.266179	
0.9	0.02	0.055092	0.038663	0.038622	0.038651
	0.01	0.043197	0.038638	0.038633	
1.0	0.02	0.003517	0.000902	0.000911	0.000912
	0.01	0.001385	0.000911	0.000912	
1.1	0.02	0.000137	0.000012	0.000013	0.000013
	0.01	0.000026	0.000013	0.000013	

Table 5: Error norms of Example 2 at $t = 2.4$, using $\nu = 0.005$.

Scheme	Δx	Δt	\mathbf{d}	ℓ_1	ℓ_2	ℓ_∞
LG	0.02	0.035	0.4375	$1.77\text{e} - 02$	$2.86\text{e} - 02$	$5.55\text{e} - 02$
	0.02	0.020	0.2500	$3.09\text{e} - 02$	$4.85\text{e} - 02$	$9.10\text{e} - 02$
	0.01	0.020	1.0000	$7.82\text{e} - 03$	$1.30\text{e} - 02$	$2.56\text{e} - 02$
	0.01	0.005	0.2500	$3.12\text{e} - 02$	$4.91\text{e} - 02$	$9.18\text{e} - 02$
CG	0.02	0.035	0.4375	$2.78\text{e} - 04$	$3.95\text{e} - 04$	$8.24\text{e} - 04$
	0.02	0.020	0.2500	$8.78\text{e} - 05$	$1.48\text{e} - 04$	$3.98\text{e} - 04$
	0.01	0.020	1.0000	$6.89\text{e} - 05$	$9.10\text{e} - 05$	$1.77\text{e} - 04$
	0.01	0.005	0.2500	$1.71\text{e} - 04$	$2.01\text{e} - 04$	$3.86\text{e} - 04$
QG	0.02	0.035	0.4375	$3.91\text{e} - 04$	$5.41\text{e} - 04$	$1.01\text{e} - 03$
	0.02	0.020	0.2500	$1.31\text{e} - 04$	$1.67\text{e} - 04$	$3.04\text{e} - 04$
	0.01	0.020	1.0000	$8.39\text{e} - 05$	$1.09\text{e} - 04$	$2.01\text{e} - 04$
	0.01	0.005	0.2500	$3.31\text{e} - 04$	$3.81\text{e} - 04$	$6.41\text{e} - 04$

Example 3. Burgers' equation (Eq. 1.1) with a step initial condition at $x = 0$ is used to study both the stability and parallel scalability of the integral-like method. The exact solution for infinite boundary conditions $u(-\infty, t) = 1$ and $u(\infty, t) = 0$ is

$$u(x, t) = \frac{\operatorname{erfc}\left(\frac{x-t}{2\sqrt{\nu t}}\right)}{\operatorname{erfc}\left(-\frac{x}{2\sqrt{\nu t}}\right) \exp\left(\frac{x-t/2}{2\nu}\right) + \operatorname{erfc}\left(\frac{x-t}{2\sqrt{\nu t}}\right)} \quad (5.9)$$

which becomes a traveling-wave solution thereafter about $t = 10$. Using $\nu = 1$, $\Delta x = 0.6$ and $\Delta t = 0.04$, the results are shown in Figure 5 and 6 for different experimental setups.

In Figure 7, the ℓ_2 error norm is plotted against the non-dimensional diffusion number $d = \nu \Delta t / \Delta x^2$. It can be seen that the stability condition of the integral-like method is not $d < 1$, as also indicated by Figure 2 and 4, but rather $d > 0.02$. This finding demonstrates that, unlike most simple explicit methods, the integral-like method is stable at large Δt . On the other hand, the condition $d > 0.02$ implies that the marginal range 5σ has to be larger than the grid spacing, as discussed in Section 3. The remaining problem encountered when ν is very small can be resolved by simply increasing Δt .

A weak-scaling experiment was performed on the TARA cluster of the NSTDA supercomputer center (ThaiSC) to test the parallel efficiency of the integral-like method. Both the number of grid points and the number of

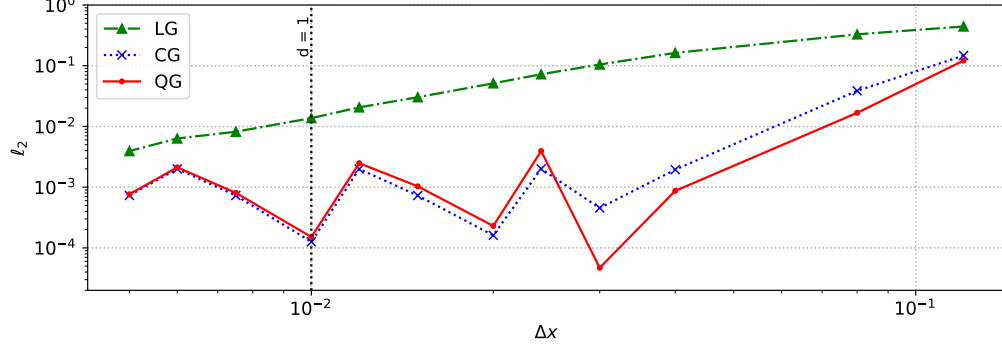


Figure 4: ℓ_2 error norm of Example 2 as a function of Δx using $\nu = 0.005$, $\Delta x = 0.02$, $\Delta t = 0.02$ and $n_t = 100$

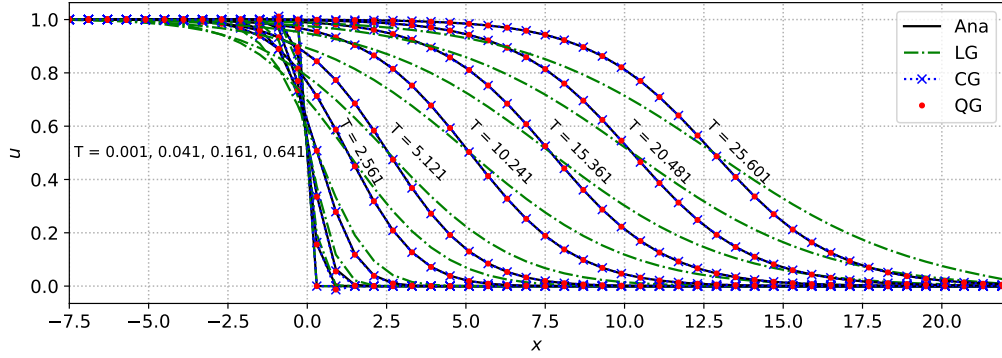


Figure 5: Numerical solutions and exact solution of Example 3: $\nu = 1$, $\Delta x = 0.6$ and $\Delta t = 0.04$

time steps are adjusted to scale computation workload while having the grid spacing Δx and the marginal range $5\sigma = 5\sqrt{2\nu\Delta t}$ approximately unaltered. In other words, roughly the same number of $u(x_j, t)$ is used in updating $u(x_i, t + \Delta t)$.

With N_s representing a running variable, the number of employed CPU cores is $N_{\text{core}} = N_s^2$ operating on the total number of grid points $n_x = 500N_s + 1$ for domain $[-15, 400N_s + 20]$ to run the simulation from $t_0 = 10$ to $t = 800N_s + 10$. The time step size Δt is varied to explore the influence of the marginal range on parallel scalability. This is because the bigger the marginal range is, the larger the overlapped areas of the domain decomposi-

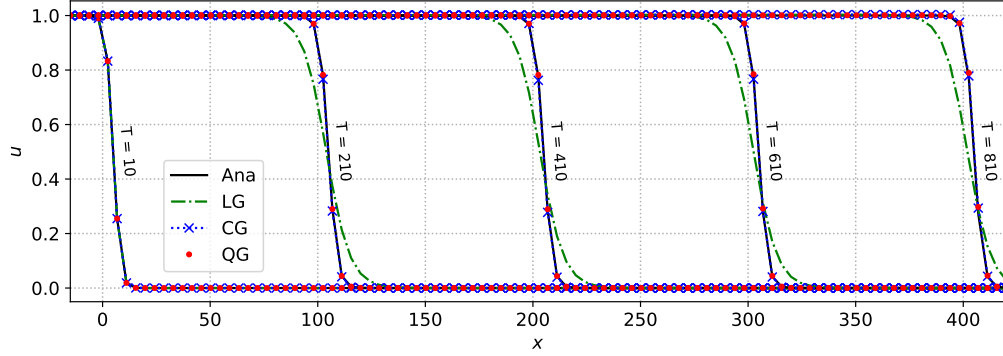


Figure 6: Numerical solutions and exact solution of Example 3: $\nu = 1$, $\Delta x = 4.35$ and $\Delta t = 0.8$

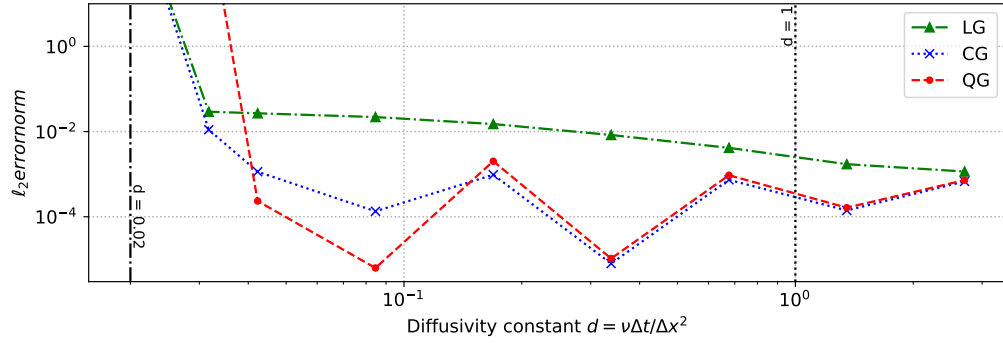


Figure 7: ℓ_2 error norm of Example 3 as a function of ν using $\Delta x = 4.35$, $n_x = 401$, $\Delta t = 0.8$ and $n_t = 100$

tion algorithm are. The outputs are shown in Figure 6.

TARA compute nodes, equipped with two Intel Xeon Gold 6148 CPU (2.40GHz) and 192GB of RAM, are employed. Our program was coded in Python and parallelized using mpi4py library, before being ported to C language by using Cython and compiled on TARA using foss-2021b toolchain. The weak-scaling parallel efficiency $R(1)/R(N_s)$, where $R(N_s)$ is wall-clock runtime of the N_s scaled case, is plotted in Figure 8 from $N_s = 1$ to $N_s = 10$. The results of the serial runtime $R(1)$ are provided in Table 6.

From Figure 8, the parallel efficiency of the integral-like schemes decreases as a larger time step size Δt is chosen. However, from Table 6, the wall-clock

Table 6: The wall-clock serial runtime $R(1)$ of each integral-like scheme for different time step size Δt , but ran for the same simulation time, i.e., from $t_0 = 10$ to $t = 810$.

Δt	5σ	d	Runtime (sec)		
			LG	CG	QG
0.2	3.16	0.26 – 0.31	1,945	3,171	4,714
0.8	6.32	1.05 – 1.23	890	1,420	2,069
3.2	12.65	4.22 – 4.92	327	508	757

runtime for a larger time step size is evidently lower. The parallel efficiency also declines as the problem size becomes larger and more CPU cores are used, but remains roughly unchanged at moderate-to-large scale cases. Therefore, the time step size of operational applications may need to be experimentally found to match available computational resources.

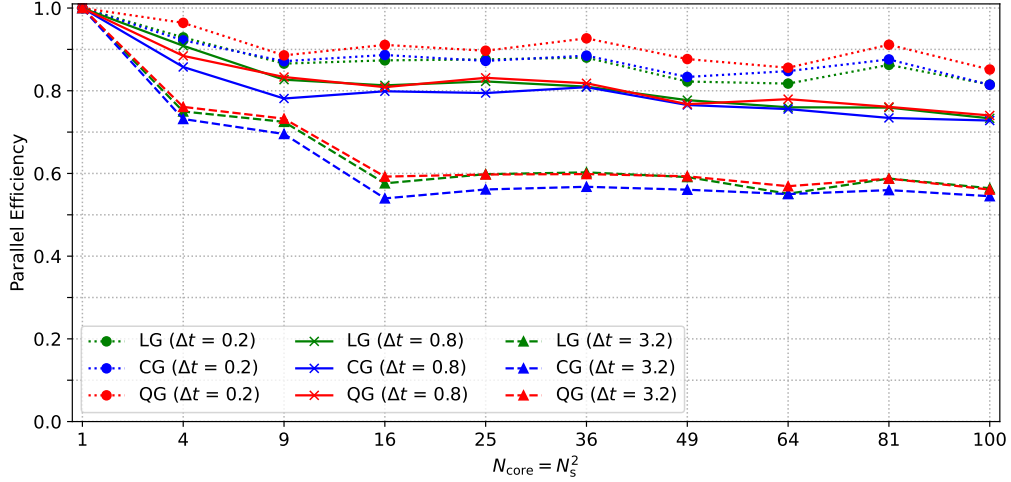


Figure 8: Weak-scaling parallel efficiency of the integral-like schemes for Burgers' equation using time step size $\Delta t = 0.2, 0.8$ and 3.2 .

Example 4. Burgers'-Fisher equation

$$\frac{\partial u}{\partial t} + u \frac{\partial u}{\partial x} = \nu \frac{\partial^2 u}{\partial x^2} - 3u(1-u)(1-2u) \quad (5.10)$$

is considered to show a possible extension of the integral-like method. Applying the split approach, which separates terms in the equation into stages and successively solve them, to Eq. (5.10), the stage equations are

$$\frac{\partial u}{\partial t} + u \frac{\partial u}{\partial x} = \nu \frac{\partial^2 u}{\partial x^2} \quad (5.11)$$

$$\frac{\partial u}{\partial t} = -3u(1-u)(1-2u) \quad (5.12)$$

The first stage, Eq. (5.11), is to solve the Burger's equation; therefore, the procedures discussed in previous sections are directly employed. The second stage, Eq. (5.12), is a growth/decay equation. Its analytical solution is found by solving

$$-3 dt = \left(\frac{1}{u} - \frac{1}{(1-u)} + \frac{4}{(1-2u)} \right) du \quad \rightarrow \quad A e^{-3t} = \frac{1}{4} - \frac{1}{4(2u-1)^2}$$

Therefore, the integral-like scheme for this second stage is

$$u(x_i, t+\Delta t) = \frac{1}{2} \left(1 \pm \frac{1}{\sqrt{1-4A \exp(-3\Delta t)}} \right) \quad \text{where} \quad A = \frac{1}{4} \left(1 - \frac{1}{(2u(x_i, t) - 1)^2} \right)$$

From [41], an exact solution of Eq. (5.10) when $\nu = 1$ is

$$u(x, t) = \frac{1}{2} \left(1 - \tanh \left(x - \frac{t}{2} \right) \right) \quad (5.13)$$

Using the same setup as in Figure 5 of Example 3, the numerical results of CG and QG agree well with the exact solution as seen in Figure 9. The integral-like approach, therefore, has the potential for solving other Burger's-type equations as well.

6. Conclusions

In this study, a numerical approach based on the continuous representation of variables using local polynomial interpolation is explored. When

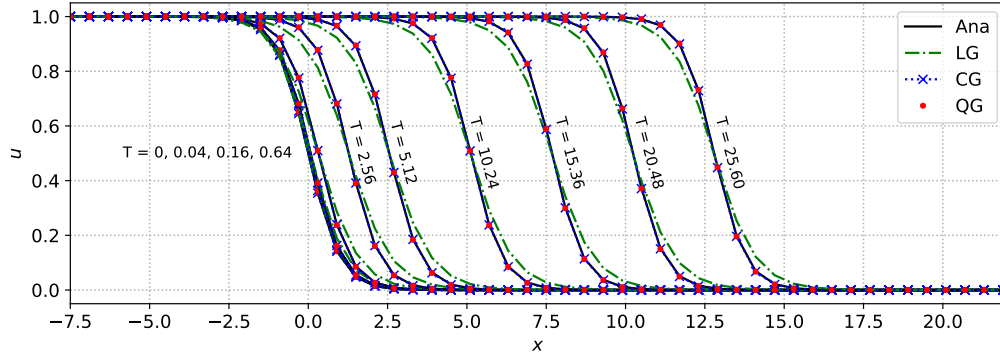


Figure 9: Numerical solutions and exact solution of Example 4: $\nu = 1$, $\Delta x = 0.6$ and $\Delta t = 0.04$

applied to solve the one-dimensional Burgers' equation, the schemes derived using linear (LG), cubic (CG) and quintic (QG) interpolations are found to be numerically stable at large time step size Δt , with a stability condition of $\nu \Delta t > 0.02 \Delta x^2$. However, the order of accuracy is not consistently improved when a smaller grid spacing is employed; nonetheless, the smallest possible error norms are around the order of 10^{-4} . Being an explicit scheme, their weak-scaling parallel efficiency is generally adequate. This approach shows promise for operational applications that favor reliability, fast computation and good parallel scalability, such as numerical weather prediction.

Acknowledgments

I would like to thank NSTDA supercomputer center (ThaiSC) for providing computational resources for this work.

References

- [1] M. P. Bonkile, A. Awasthi, C. Lakshmi, V. Mukundan, V. S. Aswin, A systematic literature review of burgers' equation with recent advances, *Pramana* 90 (2018) 1–21. doi:<https://doi.org/10.1007/s12043-018-1559-4>.
- [2] M. Abdullah, M. Yaseen, M. De la Sen, An efficient collocation method based on Hermite formula and cubic B-splines for numerical solution

- of the Burgers' equation, *Math. Comput. Simulation* 197 (C) (2022) 166–184. doi:[10.1016/j.matcom.2022.02](https://doi.org/10.1016/j.matcom.2022.02).
- [3] A. Dogan, A galerkin finite element approach to burgers' equation, *Appl. Math. Comput.* 157 (2) (2004) 331–346. doi:<https://doi.org/10.1016/j.amc.2003.08.037>.
 - [4] I. Ganaie, V. Kukreja, Numerical solution of burgers' equation by cubic hermite collocation method, *Appl. Math. Comput.* 237 (2014) 571–581. doi:<https://doi.org/10.1016/j.amc.2014.03.102>.
 - [5] Y. Hon, X. Mao, An efficient numerical scheme for burgers' equation, *Appl. Math. Comput.* 95 (1) (1998) 37–50. doi:[https://doi.org/10.1016/S0096-3003\(97\)10060-1](https://doi.org/10.1016/S0096-3003(97)10060-1).
 - [6] P. Huang, A. Abduwali, The modified local crank–nicolson method for one- and two-dimensional burgers' equations, *Comput. Math. Appl.* 59 (8) (2010) 2452–2463. doi:<https://doi.org/10.1016/j.camwa.2009.08.069>.
 - [7] A. Vs, A. Awasthi, A differential quadrature based numerical method for highly accurate solutions of burgers' equation: Dqm based numerical method for burgers' equation, *Numer. Meth. Part. D. E.* 33 (07 2017). doi:[10.1002/num.22178](https://doi.org/10.1002/num.22178).
 - [8] X. Yang, Y. Ge, B. Lan, A class of compact finite difference schemes for solving the 2d and 3d burgers' equations, *Math. Comput. Simulation* 185 (2021) 510–534. doi:<https://doi.org/10.1016/j.matcom.2021.01.009>.
 - [9] Y. Guo, Y. feng Shi, Y. min Li, A fifth-order finite volume weighted compact scheme for solving one-dimensional burgers' equation, *Appl. Math. Comput.* 281 (2016) 172–185. doi:<https://doi.org/10.1016/j.amc.2016.01.061>.
 - [10] S. Gupta, V. K. Kukreja, An improvised collocation algorithm with specific end conditions for solving modified burgers equation, *Numer. Meth. Part. D. E.* 37 (1) (2021) 874–896. doi:<https://doi.org/10.1002/num.22557>.

- [11] S. R. Jena, G. S. Gebremedhin, Decatic b-spline collocation scheme for approximate solution of burgers' equation, *Numer. Meth. Part. D. E.* 39 (3) (2023) 1851–1869. doi:<https://doi.org/10.1002/num.22747>.
- [12] Y. Jiang, X. Chen, R. Fan, X. Zhang, High order semi-implicit weighted compact nonlinear scheme for viscous burgers' equations, *Math. Comput. Simulation* 190 (2021) 607–621. doi:<https://doi.org/10.1016/j.matcom.2021.06.006>.
- [13] R. K. Mohanty, J. Talwar, A new compact alternating group explicit iteration method for the solution of nonlinear time-dependent viscous burgers' equation, *Numer. Anal. Appl.* 8 (2015) 314–328. doi:<https://doi.org/10.1134/S1995423915040059>.
- [14] R. Zhang, Y. Xi-Jun, Z. Guo-Zhong, Local discontinuous galerkin method for solving burgers and coupled burgers equations, *Chin. Phys. B* 20 (11) (2011) 110205. doi:[10.1088/1674-1056/20/11/110205](https://doi.org/10.1088/1674-1056/20/11/110205).
- [15] M. K. Kadalbajoo, A. Awasthi, A numerical method based on crank-nicolson scheme for burgers' equation, *Appl. Math. Comput.* 182 (2) (2006) 1430–1442. doi:<https://doi.org/10.1016/j.amc.2006.05.030>.
- [16] R. Kannan, Z. Wang, A high order spectral volume solution to the burgers' equation using the hopf-cole transformation, *Internat. J. Numer. Methods Fluids* 69 (4) (2012) 781–801. doi:<https://doi.org/10.1002/flid.2612>.
- [17] S. S. Kumbhar, S. Thakar, Galerkin finite element method for forced burgers' equation, *J. Math. Model.* 7 (4) (2019) 445–467. doi:[10.22124/jmm.2019.13259.1265](https://doi.org/10.22124/jmm.2019.13259.1265).
- [18] S. Kutluay, A. Bahadir, A. Özdeş, Numerical solution of one-dimensional burgers equation: explicit and exact-explicit finite difference methods, *J. Comput. Appl. Math.* 103 (2) (1999) 251–261. doi:[https://doi.org/10.1016/S0377-0427\(98\)00261-1](https://doi.org/10.1016/S0377-0427(98)00261-1).
- [19] W. Liao, An implicit fourth-order compact finite difference scheme for one-dimensional burgers' equation, *Appl. Math. Comput.* 206 (2) (2008) 755–764. doi:<https://doi.org/10.1016/j.amc.2008.09.037>.

- [20] V. Mukundan, A. Awasthi, Efficient numerical techniques for burgers' equation, *Appl. Math. Comput.* 262 (2015) 282–297. doi:<https://doi.org/10.1016/j.amc.2015.03.122>.
- [21] K. Pandey, L. Verma, A. K. Verma, On a finite difference scheme for burgers' equation, *Appl. Math. Comput.* 215 (6) (2009) 2206–2214. doi:<https://doi.org/10.1016/j.amc.2009.08.018>.
- [22] K. Sakai, I. Kimura, A numerical scheme based on a solution of nonlinear advection–diffusion equations, *J. Comput. Appl. Math.* 173 (1) (2005) 39–55. doi:<https://doi.org/10.1016/j.cam.2004.02.019>.
- [23] S.-S. Xie, S. Heo, S. Kim, G. Woo, S. Yi, Numerical solution of one-dimensional burgers' equation using reproducing kernel function, *J. Comput. Appl. Math.* 214 (2) (2008) 417–434. doi:<https://doi.org/10.1016/j.cam.2007.03.010>.
- [24] G. Zhao, X. Yu, R. Zhang, The new numerical method for solving the system of two-dimensional burgers' equations, *Comput. Math. Appl.* 62 (8) (2011) 3279–3291. doi:<https://doi.org/10.1016/j.camwa.2011.08.044>.
- [25] E. Aksan, A numerical solution of burgers' equation by finite element method constructed on the method of discretization in time, *Appl. Math. Comput.* 170 (2) (2005) 895–904. doi:<https://doi.org/10.1016/j.amc.2004.12.027>.
- [26] J. Caldwell, P. Smith, Solution of burgers' equation with a large reynolds number, *Appl. Math. Model.* 6 (5) (1982) 381–385. doi:[https://doi.org/10.1016/S0307-904X\(82\)80102-9](https://doi.org/10.1016/S0307-904X(82)80102-9).
- [27] J. Caldwell, P. Wanless, A. Cook, A finite element approach to burgers' equation, *Appl. Math. Model.* 5 (3) (1981) 189–193. doi:[https://doi.org/10.1016/0307-904X\(81\)90043-3](https://doi.org/10.1016/0307-904X(81)90043-3).
- [28] Y. Chai, J. Ouyang, Appropriate stabilized galerkin approaches for solving two-dimensional coupled burgers' equations at high reynolds numbers, *Comput. Math. Appl.* 79 (5) (2020) 1287–1301. doi:<https://doi.org/10.1016/j.camwa.2019.08.036>.

- [29] G. Arora, B. K. Singh, Numerical solution of burgers' equation with modified cubic b-spline differential quadrature method, *Appl. Math. Comput.* 224 (2013) 166–177. doi:<https://doi.org/10.1016/j.amc.2013.08.071>.
- [30] M. Ghasemi, An efficient algorithm based on extrapolation for the solution of nonlinear parabolic equations, *Int. J. Nonlinear Sci. Numer. Simul.* 19 (1) (2018) 37–51. doi:[doi:10.1515/ijnsns-2017-0060](https://doi.org/10.1515/ijnsns-2017-0060).
- [31] B. K. Singh, M. Gupta, A new efficient fourth order collocation scheme for solving burgers' equation, *Appl. Math. Comput.* 399 (2021) 126011. doi:<https://doi.org/10.1016/j.amc.2021.126011>.
- [32] M. Tamsir, N. Dhiman, V. K. Srivastava, Extended modified cubic b-spline algorithm for nonlinear burgers' equation, *Beni-Suef Univ. J. Basic Appl. Sci.* 5 (3) (2016) 244–254. doi:<https://doi.org/10.1016/j.bjbas.2016.09.001>.
- [33] Y. Gao, L.-H. Le, B.-C. Shi, Numerical solution of burgers' equation by lattice boltzmann method, *Appl. Math. Comput.* 219 (14) (2013) 7685–7692. doi:<https://doi.org/10.1016/j.amc.2013.01.056>.
- [34] N. Kumar, R. Majumdar, S. Singh, Predictor–corrector nodal integral method for simulation of high reynolds number fluid flow using larger time steps in burgers' equation, *Comput. Math. Appl.* 79 (5) (2020) 1362–1381. doi:<https://doi.org/10.1016/j.camwa.2019.09.001>.
- [35] F. M. de Lara, E. Ferrer, Accelerating high order discontinuous galerkin solvers using neural networks: 1d burgers' equation, *Comput. & Fluids* 235 (2022) 105274. doi:<https://doi.org/10.1016/j.compfluid.2021.105274>.
- [36] R. Bridson, *Fluid Simulation for Computer Graphics*, Second Edition, Taylor & Francis, 2015.
- [37] P. Olver, *Introduction to Partial Differential Equations*, Undergraduate Texts in Mathematics, Springer International Publishing, 2013.
- [38] M. Stone, P. Goldbart, *Mathematics for Physics: A Guided Tour for Graduate Students*, Cambridge University Press, 2009.

- [39] M. Sarboland, A. Aminataei, On the numerical solution of one-dimensional nonlinear nonhomogeneous burgers' equation, J. Appl. Math. 2014 (2014) 598432:1–598432:15.
- [40] E. R. Benton, G. W. Platzman, A table of solutions of the one-dimensional burgers equation, Quart. Appl. Math. 30 (2) (1972) 195–212.
- [41] J. Ramos, Picard's iterative method for nonlinear advection–reaction–diffusion equations, Appl. Math. Comput. 215 (4) (2009) 1526–1536. doi:<https://doi.org/10.1016/j.amc.2009.07.004>.